Research Open

Geology, Earth and Marine Sciences
Volume 7 Issue 1

Research Article

Extremely ^{13}C-rich Diamond in Orthorhombic Cassiterites in the Variscan Erzgebirge, Saxony/Germany

Rainer Thomas*

Im Waldwinkel 8, D-14662 Friesack, Germany

Corresponding author: Rainer Thomas, Im Waldwinkel 8, D-14662 Friesack, Germany

Received: January 16, 2025; **Accepted:** January 20, 2025; **Published:** January 24, 2025

Abstract

Raman studies on a large cassiterite sample from Zinnwald, E-Erzgebirge/Germany, brought some surprising results to light. To these belong the ^{13}C-rich diamonds and graphite, as well as other minerals, first and foremost as high-pressure and high-temperature orthorhombic cassiterite. Because there are also ^{12}C-rich diamonds in the root zones in a crystal present, especially in a large cassiterite crystal from Ehrenfriedersdorf, we assume at least two distinct pulses with varying isotopes of carbon (^{12}C versus ^{13}C) in the supercritical fluids (SCGF) coming from the earth's mantle. First came ^{12}C-rich and later ^{13}C-rich supercritical fluids. If so, other isotopes can also effectively be separated in supercritical fluids.

Keywords: *Raman spectroscopy, ^{13}C-rich diamond, Orthorhombic cassiterite, Variscan tin deposits, Supercritical fluids, Isotope separation*

Introduction

A presentation about the 800 years of mining activity and 450 years of geological research in the Erzgebirge/Krůsné hory region given by Breiter (2014) [1] shows, among other things, the extensive tin exploration and the origin and relationship of tin deposits with granite magmatism. According to this classic work by many scientists, there are no questions about the genesis of this type of ore deposit. It seems that all problems are solved, which is not the case. Thomas (2024a and 2024b) [2,3] has, however, shown that the origin of the Variscan tin deposits must be newly scrutinized. The first doubts came from the intensive work on the tin deposit Ehrenfriedersdorf presented in Schütze et al. (1983) [4]. However, their conclusions are not conclusive, at least speculative. The first concrete proof came from Thomas (2024a) [2]. In this publication, we will show that the proofs of mantle participation via supercritical fluids or melts up to now are no exceptions. We classify the supercritical fluids or melts according to Ni et al. (2024) [5] as supercritical geofluids (SCGF).

Sample Materials Microscopy and Raman Spectroscopy: Methodology

Sample Material

A sample from Zinnwald (Figure 1) clearly shows two parts of cassiterite composed of an opaque part (2/3 in volume) and a transparent cassiterite-brown nearby pale part (1/3 in volume). This cassiterite contains fluid inclusions that homogenized at about 386°C (see Thomas 1982) [6] in the liquid phase (with 15 equivalent % NaCl). In the black part, no fluid inclusions are present.

The pale part of cassiterite contains many small black to colorless

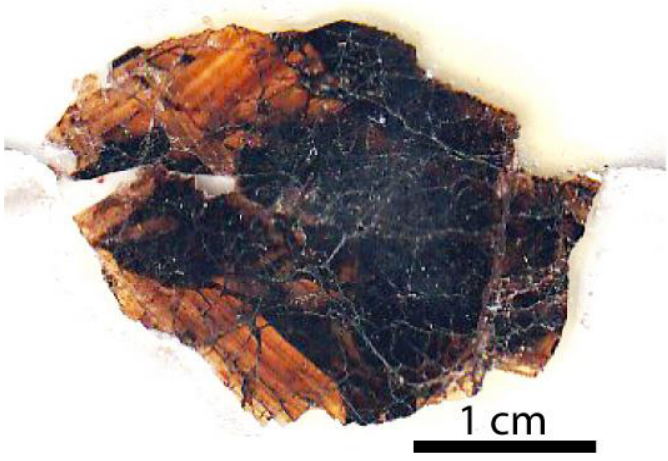

Figure 1: Cassiterite sample (Sn-23) from Zinnwald, E-Erzgebirge/Saxony. All black parts are orthorhombic cassiterite (about 2/3 in volume). The transparent brown zones contain tetragonal cassiterite parts.

(~10 µm in diameter) spherical crystals of graphite and diamond. The black part of that cassiterite contains pyrrhotine and pyrite, as well as diamond and graphite inclusions, which are relatively stable against hydrothermal activity. The sample is from the Mining Academy Freiberg. At this place, it is essential to emphasize that graphite-like material in Variscan cassiterites is typical. A description of another cassiterite sample used in this short contribution is from Ehrenfriedersdorf (Sn-70), described in Thomas 2024a [3].

Microscopy and Raman Spectroscopy

We performed all microscopic and Raman spectroscopic studies with a petrographic polarization microscope (BX 43) with a rotating

stage coupled with the EnSpectr Raman spectrometer R532 (Enhanced Spectrometry, Inc., Mountain View, CA, USA) in reflection and transmission. The Raman spectra were recorded in the spectral range of 0–4000 cm^{-1} using an up-to-50 mW single-mode 532 nm laser, an entrance aperture of 20 µm, a holographic grating of 1800 g/mm, and spectral resolution ranging of 4 cm^{-1}. Generally, we used an objective lens with a magnification of 100x: the Olympus long-distance LMPLFLN100x objective (Olympus, Tokyo, Japan). The laser power on the sample is adjustable down to 0.02 mW. The Raman band positions were calibrated before and after each series of measurements using the Si band of a semiconductor-grade silicon single-crystal. The run-to-run repeatability of the line position (based on 20 measurements each) is ±0.3 cm^{-1} for Si (520.4 ± 0.3 cm^{-1}) and 0.4 cm^{-1} for diamond (1332.7 cm^{-1} ± 0.4 cm^{-1} over the range of 80–2000 cm^{-1}). The FWHM = 4.26 ± 0.42 cm^{-1}. FWHM is the Full-Width at Half Maximum. We also used a water-clear natural diamond crystal (Mining Academy Freiberg: 2453/37 from Brazil) as a diamond reference (for more information, see Thomas et al. 2022 [7] and 2023 [8]).

Results

Diamond in Cassiterite

During the microscopic study of the cassiterite sample Sn-23 from Zinnwald, we found (besides fluid inclusions) many spherical mineral inclusions. Often, these inclusions were, according to Raman spectroscopy, diamond and/or graphite. Figure 2 shows such typical inclusion (insert right above in Figure 1) and the accompanying Raman spectrum. Conspicuously is the Raman doublet at 1309 and 1514 cm^{-1}, which is characteristically for a very ^{13}C-rich diamond (see Blank et al. 2016) [9]).

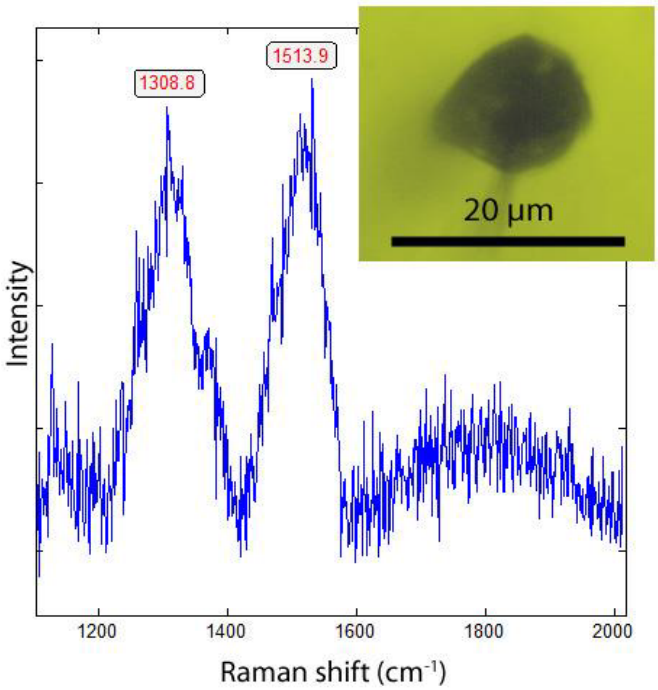

Figure 2: Raman spectrum of lonsdaleite in pale-colored cassiterite (Sn-23). The photomicrograph shows the ^{13}C-rich diamond crystal (30 µm deep) in the cassiterite matrix as well as ^{13}C-rich graphite (G-band at about 1514 cm^{-1}). The Raman spectrum was taken with 5.0 mW laser power on the sample (15 minutes exposure) – see Blank et al. 2016 [9].

Because this type of diamond and graphite is currently untypical, we have performed further Raman measurements. The results on 18 different diamond inclusions and the belonging graphite are in Table 1 compiled.

Table 1: Results on diamond and graphite in the cassiterite (Sn-23) from Zinnwald and references.

Mineral	First-order Raman line (cm^{-1})	FWHM (cm^{-1})	n (number of crystals)
^{13}C-rich Diamond	1313.9 ± 6.1	59.4 ± 19.1	18
^{12}C-rich Diamond[1)]	1332.7 ± 0.4	4.26 ± 0.42	20
^{13}C-rich Graphite	1521.5 ± 8.5	70.0 ± 26.0	10
^{13}C-rich Gr needle	1518.8 ± 1.1	39.3 ± 14.7	6
^{12}C-rich Graphite[2)]	1581.5	3.5	-
^{13}C-rich Graphite[2)]	1519.0	-	-

1) See Methodology

2) According to Gutierrez et al. 2014 [10] and Thomas et al. (2021) [11].

3) Gr – graphite (about 73 µm deep)

Besides the diamonds with a marked G-band at about 1522 cm^{-1}, there are also diamonds without such a G-band (Figure 3).

Figure 4 shows a Raman spectrum of ^{13}C-rich diamond with an outlined ^{13}C-rich graphite G band at 1527 cm^{-1}.

Figure 5 shows the relationship between the laser energy on the sample and the band position of the first-order diamond band. We see clearly that the values at the low energy (0.92 mW) represent the best values for the estimation of the ^{13}C concentration. The data in Figure 5 shows a linear correlation: Band position = 1310.53 + 0.16871

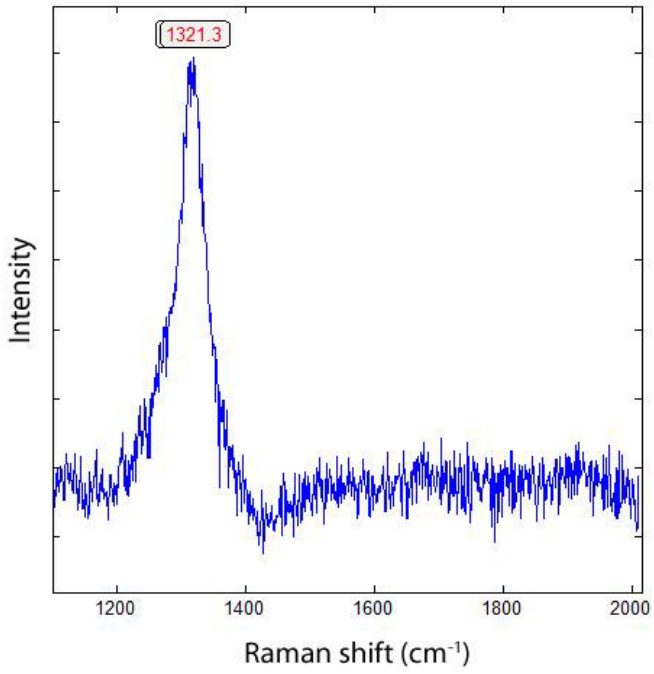

Figure 3: ^{13}C-rich diamond in cassiterite (Sn-23) from Zinnwald without graphite band. The Raman spectrum was taken with 1.0 mW laser power on the sample (15 minutes exposure).

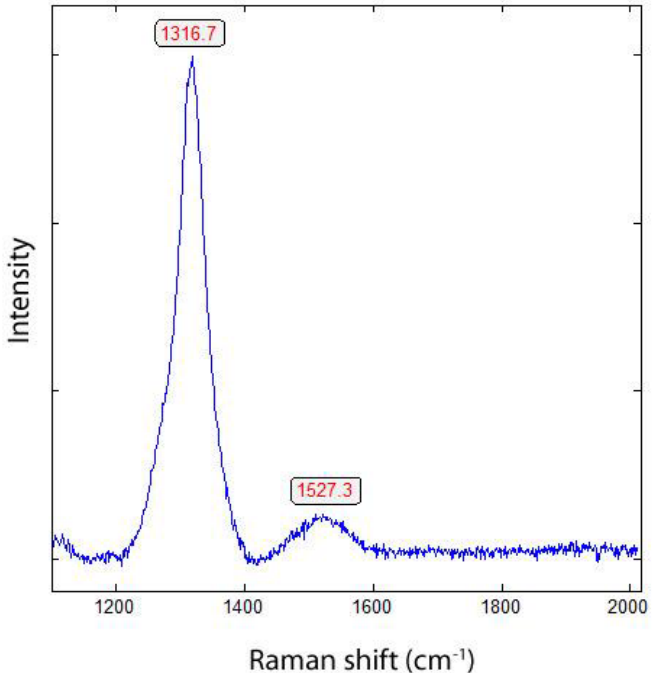

Figure 4: Raman spectrum of ^{13}C-rich diamond in cassiterite (Sn-23) from Zinnwald (30 mW on sample). The Raman band at 1527 cm^{-1} is the G band from the ^{13}C-rich graphite (see Gutierrez et al. (2014) [10]).

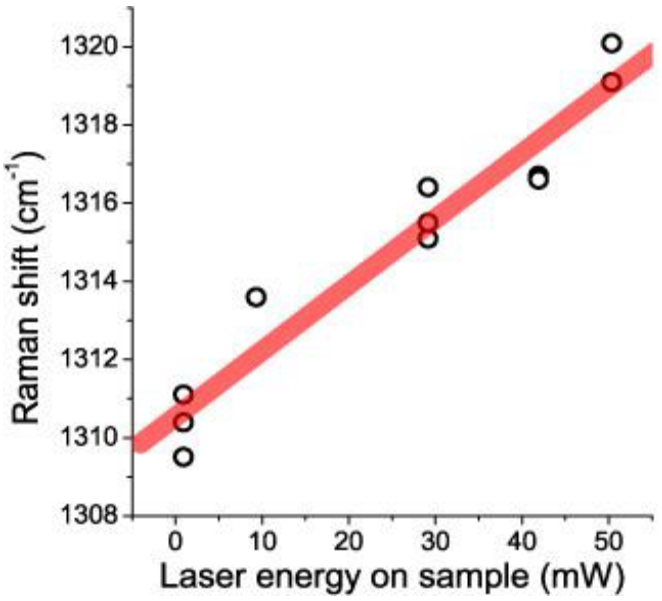

Figure 5: Correlation of the Raman shifts with the laser energy used on the sample.

* mW. The extrapolation to the lowest value of 0.92 mW results in a value of 1310.7 cm^{-1}. According to Anthony and Banholzer (1992), the first-order Raman peak position has a ^{13}C content of the diamond of about 50%. For a natural diamond that is very high, and if we assume that this diamond represents the quasi-frozen state from the deep, it follows, according to Schiferl et al. (1997) [12], a minimum pressure of about 7 GPa.

Orthorhombic Cassiterite Bearing ^{13}C-rich Diamond

The relatively large cassiterite crystal aggregate (Figure 1) from Zinnwald/Erzgebirge/Germany, sample Sn-23, contains large parts of different orthorhombic cassiterites. Tetragonal cassiterite is not present or only in traces in the whole sample Sn-23. It is well known that the polymorphs of cassiterite can easily be transformed into another (Balakrishnan et al., 2022) [13]. Therefore, different polymorphs can be present side by side, which makes the differentiation difficult. Figure 6 is an example of a more tetragonal cassiterite (with dominant indications of the Pbcn-type: 75.0, 124.8, 245, and 472.6 cm^{-1}). The strong Raman band at 75.0 cm^{-1} is untypical for tetragonal cassiterite (see Figure 5 in Thomas 2024b) [3].

Figure 7 shows the Raman spectrum of more dark cassiterite from the center of the plate (Sn-23 from Zinnwald). The strong band at 75.0 cm^{-1} corresponds, according to Thomas 2024b, to a pressure of about 10.5 GPa.

The very strong Raman band 121.4 cm^{-1} (122.7 ± 1.02 cm^{-1}; n = 6) results in a pressure of 21.9 GPa (see also Helwig et al. 2003 [14] and Thomas 2024b [3]). By the mixture of different parts of high-pressure and high-temperature SnO_2 polymorphs of rutile-type→**$CaCl_2$-type → pyrite-type → ZrO_2 orthorhombic phase I → cotunnite-type** (Balakrishnan et al. (2022) [13] and Shieh et al. (2006) [15]) demonstrate that high-pressure phases ($CaCl_2$- and cotunnite-type) are essential pieces of evidence for the transport of this ore mineral from mantle depths to the crust region. The presence of ^{13}C-rich diamonds in all parts of this Zinnwald cassiterite sample (Sn-23) supports this statement. Noteworthy is also the general presence of graphite and traces of Fe, Ta, Nb, Ti, Mn, Fe, and Zr (Betechtin, 1964) [16], which make the determination of the polymorphs of cassiterite a little bit difficult by the shift of the Raman bands.

Interpretation

The clear evidence of ^{13}C-rich diamonds in orthorhombic cassiterite from Zinnwald demonstrates clearly that a lot of cassiterite

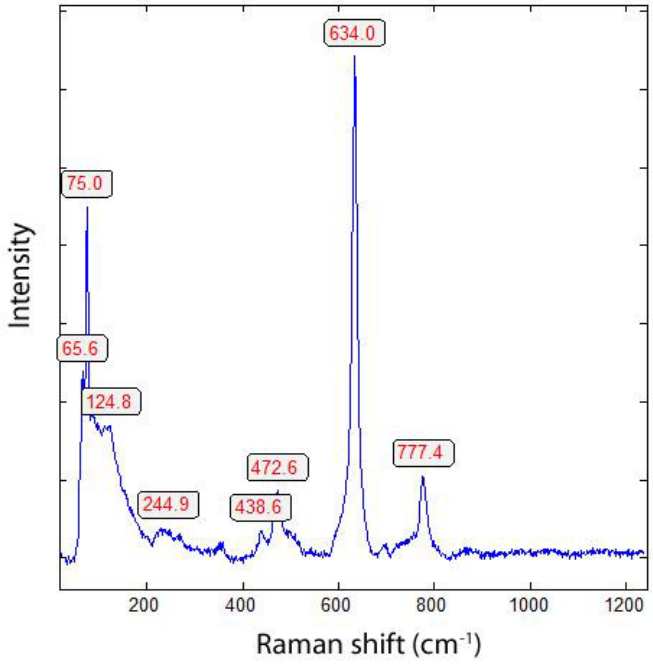

Figure 6: Raman spectrum of light cassiterite from the edge of sample (Sn-23).

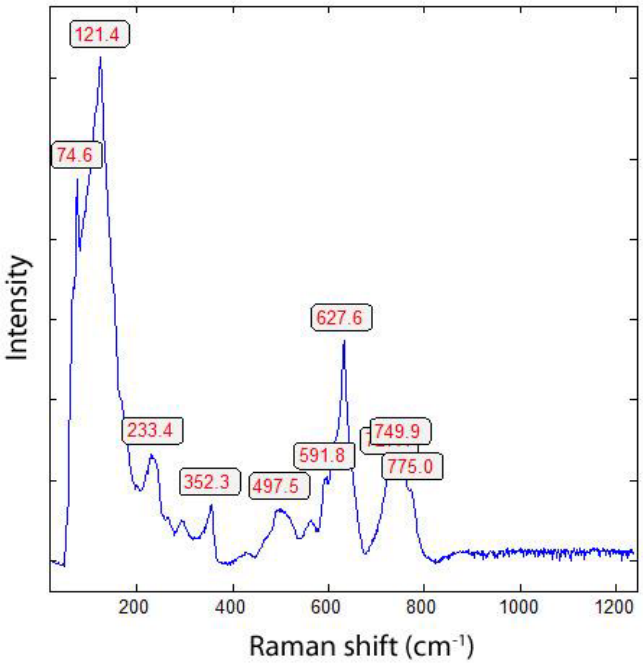

Raman spectrum of dark cassiterite from the center of the crystal plate (Sn-23 from Zinnwald).

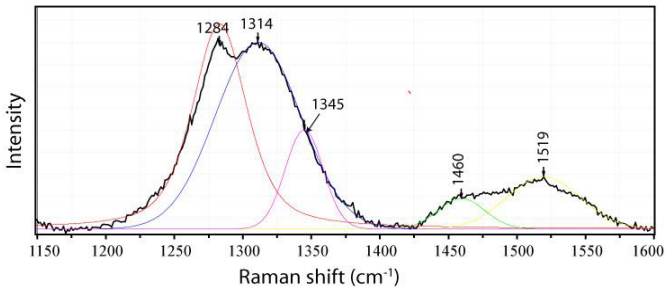

Figure 8: Raman spectrum of diamond in orthorhombic cassiterite from Ehrenfriedersdorf – sample Sn-70 (size 4 x 2 cm). The Raman band at 1284 cm^{-1} corresponds to an almost isotopic pure ^{13}C diamond, which is according to Enkovich et al. 2016 at 1283.1 cm^{-1}. The G-band is at 1519 cm^{-1}.

or tin comes directly from the mantle range. The old genetic thinking about the origin of the Variscan tin deposits of the Erzgebirge/Germany alone from the surrounding granite is, therefore, questionable.

Up to now, we have found mainly ^{12}C-rich diamonds in cassiterite (Thomas 2024a, 2024b – [2,3] and Thomas and Rericha 2025) – [17] from Ehrenfriedersdorf in the Central Erzgebirge/Germany, in the cotunnite-type cassiterite from Krupka (Krušné hory Mining District/ Czech Republic, and the Slavkovský les, North Bohemia (Czech Republic). Figures 2 and 4, as well as Table 1, clearly show that the diamond in the here-discussed case is ^{13}C-rich because the typical G band of graphite lies at significantly lower values. That is also valid for the main crystal of cassiterite Sn-70 from Ehrenfriedersdorf in the central Erzgebirge.

Table 2 shows the measured data on the ^{13}C-rich diamond in cassiterite from Ehrenfriedersdorf, Central Erzgebirge, Germany, as well as the data for isotope pure diamond and graphite according to Enkovich et al. (2016) – [18] and Gutierrez et al. (2014) – [10].

Table 2: Raman bands of ^{13}C- and ^{12}C-rich diamonds and graphite, according to Gutierrez et al. (2014) [10] and Enkovich et al. (2016) [18]. The values for the diamonds in cassiterite from the Sauberg mine near Ehrenfriedersdorf (Sn-70) are based on this work (6 crystals).

	^{13}C-rich diamond	**^{12}C-rich diamond**	**^{13}C-rich graphite**	**^{12}C-rich graphite**
Pure ^{13}C phase	1283.1 cm^{-1}	-	1519 cm^{-1}	-
Pure ^{12}C phase		1332.7 cm^{-1}		1581 cm^{-1}
Sn-70	1286.7 ± 6.5 cm^{-1}	1318.8 ± 0.9 cm^{-1}	1518.1 ± 0.8 cm^{-1}	-

From a first approximation, according to Enkovich et al. (2016) [18], the ^{12}C-richer cassiterite Sn-70 has a value of $^{12.6}$C ($^{12.5}$C has an isotopically mixed 1:1 composition). The finding of clear proofs for ^{13}C-rich diamond and graphite in cassiterite from Zinnwald forces the assumption of two different pulses of supercritical fluid (SCGF): the first one is in ^{12}C enriched, and the second one is in ^{13}C enriched. In the Sauberg mine near Ehrenfriedersdorf, we found diamonds in a cassiterite crystal that were very rich in ^{13}C. However, the root zone of the same crystal dominates in ^{12}C-rich diamonds (Thomas 2024a) [2].

Discussion

The presence of orthorhombic cassiterite up to the cotunnite polytype, as well as the frequent occurrence of ^{12}C- and ^{13}C-rich diamonds in different minerals, here in cassiterite, forces a re-thinking of the old genetic concept of the formation of the Variscan tin deposits in the Erzgebirge/Germany and the Krušné hory Mining District/Czech Republic. Furthermore, if so, other isotopes can also effectively be separated in supercritical fluids (SCGF). Also, another point is essential: with the widespread SCGFs in the whole Variscan Erzgebirge region, an enormous amount of water comes from the mantle into the crustal region.

Acknowledgment

For the samples, I thank Professor Ludwig Baumann (1929-2008) from the Mining Academy Freiberg, who initiated my interest in the genetic aspects of the Variscan tin deposits, too. Paul Davidson (Hobart, Tasmania) and Jim D. Webster (AMNH; New York) stimulated my critical thinking regarding supercritical fluids. The nearby daily discussion with Adolf Rericha (Falkensee) forced my intense Raman work.

References

1. Breiter K (2014) 800 years of mining activity and 450 years of geological research in the Krušné Hory/Erzgebirge Mountains, Central Europe. *Bol Mus Para Emilio Goeldi. Ciências Naturais* 9: 105-134.

2. Thomas R (2024a) The $CaCl_2$-to-rutile phase transition in SnO_2 from high to low pressure in nature. *Geol Earth Mar Sci* 6: 1-4.

3. Thomas R (2024b) Rhomboedric cassiterite as inclusions in tetragonal cassiterite from Slavkovský les – North Bohemia (Czech Republic). *Geol Earth Mar Sci* 6: 1-6.

4. Schütze H, Stiehl G, Wetzel K, Beuge P, Haberland R, et al. (1983) Isotopen- und elementgeochemische sowie radiogeochronologische Aussagen zur Herkunft des Ehrenfriedersdorfer Granits. - Ableitung erster Modellvorstellungen. *ZFI-Mitteilungen.* 76: 232-254.

5. Ni H, Xiao Y, Xiong X, Liu X, Gao C, et al. (2024) Formation and evolution of supercritical geofluid. *Science China Earth Sciences*. 67: 1-13.

6. Thomas R (1982) Ergebnisse der thermobarometrischen Untersuchungen an Flussigkeitseinschlussen in Mineralen der postmagmatischen Zinn-Wolfram-Mineralisation des Erzgebirges. Freiberger Forschungshefte C370, Pg: 85.

7. Thomas R, Davidson P, Rericha A, Recknagel U (2022) Water-rich coesite in prismatine-granulite fromWaldheim/Saxony. Veröffentlichungen Naturkunde Mus. *Chemnitz*. 45: 67-s80.

8. Thomas R, Davidson P, Rericha A, Recknagel U [2023] Mineral inclusions in a crustal granite: Evidence for a novel transcrustal transport mechanism. *Geosciences*. 13.

9. Blank VD, Kulnitsky BA, Rerezhogin IA, Tyukalova EV, Denisov VN, et al. (2016) Graphite-to-diamond (^{13}C) direct transition in a diamond anvil high-pressure cell. *Int. J. Nanotechnol.* 13: 604-611.

10. Gutierrez G, Le Normand F, Aweke F, Muller D, Speisser C, et al. (2014) Mechanism of thin layers graphite formation by 13C implantation and annealing. *Appl Sci.* 4: 180-194.

11. Thomas R, Rericha A, Davidson P, Beurlen H (2021) An unusual paragenesis of diamond, graphite, and calcite: A Raman spectroscopic study. *Estudos Geológicos* 31: 3-15.

12. Schiferl D, Malcolm N, Zaug JM, Sharma SK, Cooney TF, et al. (1997) The diamond ^{13}C/^{12}C isotope Raman pressure sensor system for high-temperature/pressure diamond-anvil cells with reactive samples. *J. Appl Phys* 82: 3256-3265.

13. Balakrishnan K, Veerapandy V, Fjellvag H, Vajeeston P (2022) First-principles exploration into the physical and chemical properties of certain newly identified SnO_2 polymorphs. *ACS Publ.* 7: 10382-10393.

14. Hellwig H, Goncharov AF, Gregoryanz E, Mao H, Hemley RJ (2003) Brillouin and Raman spectroscopy of the ferroelastic rutile-to CaCl2 transition in SnO2 at high pressure. *Physical Review B* 67: 174110-1174110-7.

15. Shieh SR, Kubo A, Duffy TS, Prakapenka VB, Shen G (2006) High-pressure phases in SnO_2 to 117 GPa. *Phys. Rev. B* 73: 014105-1–014105-7.

16. Betechtin AG (1964) Lehrbuch der speziellen Mineralogie. VEB Deutscher Verlag für Grundstoffindustrie, Leipzig, PG: 679.

17. Thomas R, Rericha A (2025) Extreme element enrichment by the interaction of supercritical fluids from the mantle with crustal rocks. *Minerals*. 15: 1-10.

18. Enkovich PV, Brazhkin VV, Lyapin SG, Novikov AP, Kanada H, et al. (2016) Raman spectroscopy of isotopically pure (^{12}C, ^{1}3C) and isotopically mixed ($^{12.5}$C) diamond single crystals at ultrahigh pressures. *Journal of Experimental and Theoretical Physics.* 123: 443-451.

Citation:

Thomas R (2025) Extremely ^{13}C-rich Diamond in Orthorhombic Cassiterites in the Variscan Erzgebirge, Saxony/Germany. *Geol Earth Mar Sci* Volume 7(1): 1-5.